



# Reversible Boolean networks I: distribution of cycle lengths

S.N. Coppersmith\*, Leo P. Kadanoff, Zhitong Zhang

*James Frank Institute, The University of Chicago, 5640 S. Ellis Ave., Chicago, IL 60637, USA*

Received 8 May 2000; received in revised form 26 September 2000; accepted 10 October 2000

Communicated by E. Ott

---

## Abstract

We consider a class of models describing the dynamics of  $N$  Boolean variables, where the time evolution of each depends on the values of  $K$  of the other variables. Previous work has considered models with dissipative dynamics. Here, we consider time-reversible models, which necessarily have the property that every possible point in the state space is an element of one and only one cycle. The orbits can be classified by their behavior under time reversal. The orbits that transform into themselves under time reversal have properties quite different from those that do not; in particular, a significant fraction of latter-type orbits have lengths enormously longer than orbits that are time-reversal symmetric. For large  $K$  and moderate  $N$ , the vast majority of points in the state space are on one of the time-reversal singlet orbits, and a random hopping model gives an accurate description of orbit lengths. However, for any finite  $K$ , the random hopping approximation fails qualitatively when  $N$  is large enough ( $N \gg 2^{2^K}$ ). As in the dissipative case, when  $K$  is large, typical orbit lengths grow exponentially with  $N$ , whereas for small enough  $K$ , typical orbit lengths grow much more slowly with  $N$ . The numerical data are consistent with the existence of a phase transition at which the average orbit length grows as a power of  $N$  at a value of  $K$  between 1.4 and 1.7. However, in the reversible models, the interplay between the discrete symmetry and quenched randomness can lead to enormous fluctuations of orbit lengths and other interesting features that are unique to the reversible case. © 2001 Elsevier Science B.V. All rights reserved.

PACS: 05.40.+b; 05.45.+j; 64.60.Lx

Keywords: Gene regulatory networks; Random Boolean networks; Time-reversible Boolean networks; Cellular automata

---

## 1. Introduction

### 1.1. Review of dynamical Boolean networks

In recent years, considerable effort has been devoted to the study of the development of complexity in dynamical systems. Complexity is observed in such different examples as ecosystems (see [1]), spin glasses (see [2,21]), and quite broadly through the biological sciences [3]. One thread of activity involves the study

of the behavior of dynamical systems consisting of  $N$  variables  $\sigma_i^j$  (the site label  $j = 1, \dots, N$ ), where each  $\sigma_i^j$  is Boolean, so that it takes on one of the two values that we choose to be  $\pm 1$ . The configuration of the system at time  $t$  is characterized by a ‘state’  $\Sigma_t$ :

$$\Sigma_t = (\sigma_t^1, \sigma_t^2, \dots, \sigma_t^j, \dots, \sigma_t^N). \quad (1)$$

The time development is given by saying that the state at time  $t + 1$  is a prescribed function of the state at time  $t$ , i.e.,

$$\Sigma_{t+1} = \mathcal{M}(\Sigma_t). \quad (2)$$

---

\* Corresponding author.

E-mail address: [snc@franck.uchicago.edu](mailto:snc@franck.uchicago.edu) (S.N. Coppersmith).

The mapping can also be written

$$\sigma_{t+1}^j = F^j(\Sigma_t) \quad \text{for } j = 1, \dots, N, \quad (3)$$

where the  $F^j$  also take on the values  $\pm 1$ .

The number of different states of the system is finite; it is

$$\omega = 2^N, \quad (4)$$

and the mapping function  $\mathcal{M}$  is independent of time. Therefore, starting from any state, eventually the system falls into a cyclic behavior and follows that cycle forever.

Typically, each of the functions  $F^j(\Sigma)$  is picked so that it depends upon exactly  $K$  distinct input spin variables in the vector  $\Sigma$ . A random choice is made to determine which components  $\sigma^k$  will appear in each  $F^j(\Sigma)$ ; this fixes the ‘wiring’ of the realization. Once  $K$  and  $N$  and the assignment  $\sigma^k$ ’s are fixed, the each mapping function  $F^j(\Sigma)$  is selected at random from the set of all Boolean functions of  $K$  Boolean variables. The randomly chosen  $N$  sets of  $K$  input spin variables and the functions  $F^j$  compose a *realization*. Given an initial configuration of the system, a realization will completely define the system’s behavior. The realization is picked at the beginning of the calculation for the system and remains independent of time. Since there are  $2^{2^K}$  Boolean functions of  $K$  Boolean variables and  $\binom{N}{K}$  different ways to assign  $K$  distinct input spin variables, as  $K$  and/or  $N$  become large the number of different realizations is truly huge.

This kind of model is often called a *Kauffman net* because Kauffman [3–5] developed a program of study for generic maps of this type. Later, this program was extended by Derrida [2,21], Flyvbjerg [6], Parisi [7–9], and others [10,11,22,23]. Quantities of interest that have been studied include the distribution of cycle lengths and the number of starting points which will eventually lead to a given cycle. (These points form what is called the basin of attraction of the cycle.) One calculates the above quantities by enumeration or by Monte Carlo simulation for each realization and then averages over realizations with the same values of  $N$  and  $K$ .

The Kauffman net is said to be ‘dissipative’ since several different states may map into one. Thereby information is lost.

The behavior of Kauffman nets are interesting and surprising. Large  $K$ -values produce a complex time-behavior which closely resembles Parisi’s theory of spin glasses [2,8,12]. For large  $K$ , the cycle lengths grow exponentially with the number of spins  $N$ . Conversely for  $K = 0$  or  $1$ , the cycles tend to be short. At the ‘critical’ value,  $K = 2$ , typical cycle lengths grow as a power of  $N$ , and for large  $N$ , the probability of observing a cycle of length  $L$  varies as a power of  $L$ . (For a study of critical properties see Refs. [8,10,13].) This three-phase structure is typical of phase transition problems [14] in which an ordered and a disordered phase are separated by a critical phase line.

### 1.2. A time-reversible network

Thus, a great deal is known about the behavior of Kauffman nets, which can be viewed as a class of generic dynamical mapping problems. But not all problems are generic. For example, many of the systems considered in Hamiltonian mechanics are *reversible*. Such systems have the property that some transformation of the coordinates (e.g., changing the sign of all velocities) makes the system retrace its previous path. Thus, a forward motion and its inverse are equally possible. This paper is devoted to a study of the behavior of discrete reversible maps.<sup>1</sup>

In contrast to a dissipative system, in a finite and reversible dynamical system, every possible state is in exactly one cycle. Because one and only one state at time  $t$  maps into a predefined state at time  $t + 1$ , any cycle can be traversed equally well forward or backward. There are no basins of attraction in this kind of system. The long-term properties are then described by giving the number of cycles of length  $l$ ,  $N(l)$ .

It turns out that for the smaller values of  $K$ ,  $N(l)$  is an oscillating function of  $l$  in which the small prime divisors of  $l$  play a major role. We shall study this effect in a companion paper. For now, we focus on the

<sup>1</sup> Another model involving reversible dynamics with behavior different from ours was introduced in Ref. [15]. Related works include Ref. [24].

gross scaling properties of  $N(l)$ , by using a cumulative distribution

$$S(l) = \frac{\sum_{j=l+1}^{\infty} jN(j)}{\sum_{k=1}^{\infty} kN(k)}, \quad (5)$$

which gives the probability of finding a cycle of length greater than  $l$  by picking the realizations and the initial cycle element at random. We call  $S(l)$  a “survival probability”.

### 1.2.1. Definition of the model

We construct our time-reversible maps using the method of two time slices that was studied for discrete systems by Fredkin and collaborators [16].<sup>2</sup>

As in the usual dissipative Kauffman model, our basic variable is a list,  $\Sigma$ , of the  $N$  ‘spin variables’,  $\sigma^j$ :

$$\Sigma = (\sigma^1, \sigma^2, \dots, \sigma^j, \dots, \sigma^N). \quad (6)$$

The value of  $\Sigma$  is given for each integer value of the time, and written as  $\Sigma_t$ . In our reversible mappings, the spin configuration at time  $t + 1$ ,  $\Sigma_{t+1}$ , depends upon  $\Sigma_t$  and  $\Sigma_{t-1}$  according to the rule

$$\sigma_{t+1}^j = \sigma_{t-1}^j F^j(\Sigma_t), \quad (7)$$

where the  $F$ ’s are picked exactly as in the dissipative Kauffman net. Since the  $\sigma$ ’s take on the values  $\pm 1$ , our model can be written in the equivalent form

$$\sigma_{t+1}^j \sigma_{t-1}^j = F^j(\Sigma_t), \quad (8)$$

which exhibits a quite manifest time-reversal invariance. The models given by Eq. (7) are the subject of this paper.

The information needed to predict future time steps is called the *state* of the system. In our case, the state

at time  $t$ ,  $\mathcal{S}_t$ , is given by two time slices or *substates*  $\Sigma_t$  and  $\Sigma_{t-1}$  as

$$\mathcal{S}_t = \begin{pmatrix} \Sigma_{t-1} \\ \Sigma_t \end{pmatrix}, \quad (9)$$

and the full mapping is of the form

$$\mathcal{S}_{t+1} = \mathcal{M}(\mathcal{S}_t). \quad (10)$$

The history of the system is given by listing the substates in order as

$$\Sigma_0, \Sigma_1, \Sigma_2, \dots, \Sigma_n.$$

If there are  $N$  spins, the volume of the state space is

$$\Omega = 2^{2N} = \omega^2. \quad (11)$$

Since the dynamics are deterministic,  $\Omega$  gives the length of the longest possible cycle. However, as we shall see, that length is never attained.

### 1.3. Questions to be asked

This paper concerns the distribution of cycle lengths in the time-reversible models. Fig. 1 shows plots of probabilities of observing a cycle of length larger than  $l$  for systems with  $N = 10$  and various  $K$ , averaged over realizations. For  $K = 1$ , the cycles are very short; for  $K = N$ , they have a wide range of lengths, but the longest ones have length of order  $2^N$ , much less than the number of points in the state space,  $2^{2N}$ . For  $K = 2$ , a wide range of cycle lengths is seen, including some lengths which considerably exceed the ones in the  $K = N$  system. For smaller values of  $K$ , the number of cycles of length  $l$  tends to be a strongly oscillatory function of  $l$ . We shall discuss this oscillation in a subsequent publication.

To understand these results for the cycle lengths, we shall need to understand in some detail the interplay between the quenched randomness of the system and the time-reversal symmetry. We will find that the cycles can be divided into two classes, those that are symmetric under time-reversal and those that are not. There are profound differences between the behaviors of these two types of cycles.

The companion paper will discuss the growth of the ‘Hamming distance’ between configurations, defined

<sup>2</sup> The construction of time-reversible models by using variables from two different times has a long history. Imagine doing a calculation in ordinary classical mechanics using small but discrete time steps. The behavior depends upon the position and velocity of each particle, but one might wish to do the analysis in terms of positions alone. To do this, one works with a state defined by the positions at two closely neighboring times. The difference in position at the two times gives an estimate of the velocity vector. In this way, one can construct a two slice model of particle behavior.

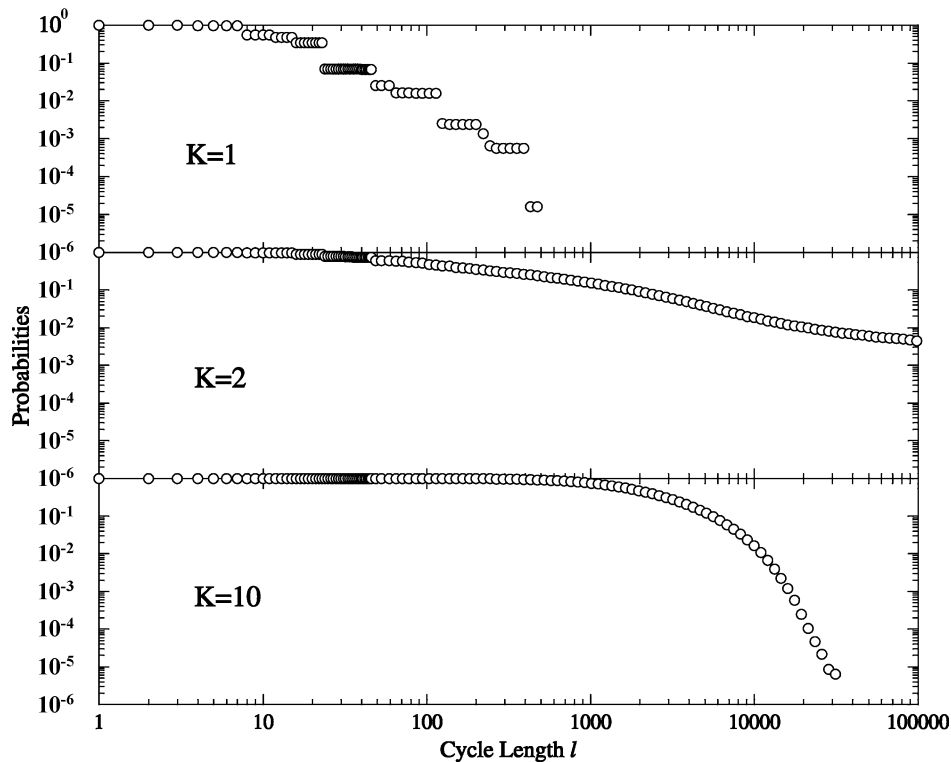


Fig. 1. Plots of probabilities of observing a cycle of length greater than  $l$  as a function of  $l$  for  $N = 10$  and  $K = 1, 2,$  and  $N$ . These plots are derived from simulations which average over 10,000 realizations for each value of  $K$ . For each realization, one initial state randomly chosen from the state space was examined.

as the the number of Boolean variables which are unequal in the two configurations. We shall compare two configurations that initially differ by a single spin flip, and see how this distance depends upon the number of iterations. For small  $K$ , the growth in the distance may be very slow; for large  $K$ , we see much more rapid growth.

Our simulational data of cycle length distributions suggest but do not prove the existence of phase transition. However, in the companion publication, we shall see that the behavior of the Hamming distance can be used to demonstrate convincingly the presence of a type of percolation transition at a value of  $K$  of about 1.6.

#### 1.4. Outline of the rest of paper

In the next section, we discuss some special features of time-reversible models and their implications

for classifying different kinds of cycles. The section after that is devoted to the limiting cases,  $K = 0$  and  $N$ . Section 4 describes the structures seen at intermediate  $K$ . Appendices A and B cover some more peripheral issues.

## 2. Time-reversal invariance

At first sight, it is not obvious that time-reversal invariance should have any important effect on the distribution of cycle lengths. However, Birkhoff [17] and later Greene [18,25] and others [19] showed one important mechanism by which the time-reversal process works to set the cycle length.

### 2.1. Symmetry points

In our model, there are special points in the phase space which we might call *mirrors*. A mirror produces

a time-reflected motion in the sequence, e.g.,

$$\dots, \Sigma_3, \Sigma_2, \Sigma_1, \Sigma_1, \Sigma_2, \Sigma_3, \dots, \quad (12a)$$

or, as another example

$$\dots, \Sigma_3, \Sigma_2, \Sigma_1, \Sigma_0, \Sigma_1, \Sigma_2, \Sigma_3, \dots. \quad (12b)$$

We call the first type (Eq. (12a)) a *twin* configuration and the second type (Eq. (12b)) a *sandwich* configuration. The phase space contains many of these mirrors. A typical and important cyclic motion is for the sequence of substates to hit a mirror, be reflected, hit another mirror, be reflected once more, and thereby be forced into a cyclic behavior.

More explicitly, if we record an orbit of the time-reversible model using a sequence of substates, e.g.,  $\dots, \Sigma_{t-1}, \Sigma_t, \Sigma_{t+1}, \dots$ , we may call the state  $\mathcal{S}$ -value defined as  $\left( \begin{smallmatrix} \Sigma_t \\ \Sigma_{t+1} \end{smallmatrix} \right)$  at which  $\Sigma_{t+1} = \Sigma_t$  a twin special point, and another  $\mathcal{S}$ -value a sandwich special point if  $\Sigma_{t+2}$  in the sequence equals  $\Sigma_t$ . Thus, a twin point is any state of the form

$$\mathcal{S} = \left( \begin{array}{c} \Sigma \\ \Sigma \end{array} \right), \quad (13)$$

so that the cycle will spread out in a palindromic fashion before and after this special point in the pattern of Eq. (12a). Since the entire volume of the state space is  $\Omega = \omega^2$  and since there are  $\omega$  of these invariant points, the chance that a randomly chosen point in the state space is a twin point is  $1/\omega$ . Correspondingly, a sandwich point appears when there is some value of  $\Sigma^{(s)}$  for which

$$F^j(\Sigma^{(s)}) = 1 \quad \text{for all } j \quad (14)$$

(see Eq. (7)). A sandwich point gives rise to a sequence of the form of Eq. (12b). The number of sandwich points depends on the realization. For example, if  $F^j \equiv -1$  for any  $j$ , then there are no sandwich points at all. For a given realization, we denote the number of substates that have the property of Eq. (14) by  $m$ , and we denote each such substate by the symbol  $\Sigma_\alpha^{(s)}$ ; the  $\alpha$  label differentiates between the  $m$  different sandwich substates. Since for any substate  $\Gamma$  a state of the form

$$\mathcal{S} = \left( \begin{array}{c} \Gamma \\ \Sigma_\alpha^{(s)} \end{array} \right)$$

is a sandwich state, there must be  $m\omega$  of these sandwich states.

Appendix A discusses the properties of the sandwich points. As shown there, the average over realizations  $\langle m \rangle$  is unity. When  $K = N$  and  $N$  is large,  $m$  follows a Poisson distribution,

$$P(m) = \frac{1}{m!} e^{-1} \quad (N \rightarrow \infty). \quad (15)$$

When  $K$  is small, there are large realization-to-realization fluctuations in  $m$ , and the average over realizations of higher powers of  $m$ , e.g.,  $\langle m^2 \rangle$ , can grow rapidly as a function of  $N$ . In fact, when  $N \gg 2^{2^K}$ , the vast majority of realizations have  $m = 0$ .

## 2.2. Inversions and cycles

Two states  $\mathcal{S}$  and  $\mathcal{S}'$  are time-reversed images of one another if

$$\mathcal{S} = \left( \begin{array}{c} \Sigma_1 \\ \Sigma_2 \end{array} \right)$$

while

$$\mathcal{S}' = \left( \begin{array}{c} \Sigma_2 \\ \Sigma_1 \end{array} \right).$$

All cycles belong to one of the two classes. The first class, which we call *special cycles*, each contains at least one pair of time-reversed images of one another. The other class, called *regular cycles*, contains no such pairs. In Appendix B, we show that each special cycle of length greater than 1 contains exactly two distinct special points. Furthermore, if the points are both twins or both sandwiches, the cycle has even length; if they are of different types, the cycle length is odd.

## 2.3. Counting special points and special cycles

The arguments in Section 2.1 imply that for a given realization there are  $m\omega$  sandwich points and  $\omega$  twin points. Among them there are  $m$  points that are both twin and sandwich points (consisting of a sandwich substate followed by the same substate), all of which produce  $m$  cycles of length 1. Thus, there are  $(m+1)\omega - m$  distinct special points in the state space. The

total number of special cycles is the number derived from the points which are both twins and sandwiches,  $m$ , plus the number derived from all the other special points,  $\frac{1}{2}[(m+1)\omega - 2m]$ , yielding

$$\text{number of special cycles} = \frac{1}{2}(m+1)\omega. \quad (16)$$

The importance of these special points in determining cycle properties will become clear in the following sections.

### 3. Limiting cases

This section discusses the behavior of reversible Boolean nets for the cases  $K = 0$  and  $N$ .

#### 3.1. $K = 0$

When  $K = 0$ , the evolutions of the different  $\sigma^j$ 's are uncorrelated. Each  $\sigma_t^j$  repeats after either one, two, or four steps. (In contrast, in the Kauffman net after the first step each of the  $\sigma^j$ 's remains constant.) For large  $N$ , each system is likely to contain at least one  $\sigma^j$  with period 4. Hence cycles of period 4 will dominate.

The uncorrelated cycles of the spins produce a hamming distance which can have value 0 or 1 and has period 1, 2 or 4.

#### 3.2. $K = N$

In this part, we first review the results for the dissipative Kauffman net

$$\sigma_{t+1}^j = F^j(\Sigma_t),$$

and then proceed to discuss the time-reversible case

$$\sigma_{t+1}^j = F^j(\Sigma_t)\sigma_{t-1}^j.$$

##### 3.2.1. Dissipative case

The case in which  $K$  has its maximum value,  $K = N$ , was first analyzed for the dissipative Kauffman model by Derrida [2,21]. This case has the simplifying feature that a change of a single spin changes the input of every function  $F^j$ . Since the functions are chosen randomly, this means that every new input configuration  $\Sigma_t$  leads to an output configuration  $\Sigma_{t+1}$  that is

picked at random from the whole phase space with its volume

$$\omega = 2^N.$$

This process continues until the time  $T$  at which  $\Sigma_T = \Sigma_\tau$  for some  $\tau < T$ . After that, the system cycles repeatedly through the sequence  $\Sigma_\tau, \dots, \Sigma_{T-1}$ .

To find the distribution of orbit lengths, we first calculate  $p_n$ , the probability that starting from a randomly chosen initial state at time  $t = 0$ , the orbit closes at time  $n$ . To do this, we define  $q_n$  to be the probability that the cycle remains unclosed after  $n$  steps. The probability that a closure event occurs at time zero is  $p_0 = 0$ , and thus  $q_0 = 1$ . At the time 1, the system has a probability  $p_1 = 1/\omega$  of falling into the initial value and a probability  $q_1 = 1 - p_1$  of not doing so. At time 2, there are two possible cycle closures, since the new element can be the same as either the zeroth or the first element. Thus, the conditional probability of a closure at time two, given that the closure event did not occur at any earlier time, is  $2/\omega$ . Similarly, the conditional probability of a closure event at time  $t = n$ , given that the system has not closed at time  $t = n - 1$ , is just  $n/\omega$ . Thus, the likelihood of a cycle closure at step  $n$  is

$$p_n = \frac{n}{\omega}q_{n-1}, \quad (17a)$$

and correspondingly the  $q_n$  satisfy

$$q_n = \left(1 - \frac{n}{\omega}\right)q_{n-1}. \quad (17b)$$

The solution to Eq. (17b) with  $q_0 = 1$  is

$$q_n = \prod_{j=1}^n \left(1 - \frac{j}{\omega}\right). \quad (18)$$

We shall see that  $q_n \ll 1$  unless  $n \ll \omega$ . Therefore, we can write

$$\ln q_n = \sum_{j=1}^n \ln \left(1 - \frac{j}{\omega}\right), \quad (19)$$

and expand the right-hand side for small  $j/\omega$ , yielding<sup>3</sup>

<sup>3</sup>One can also write  $q_n = \omega^{-n}\omega!/(\omega - n)!$  and expand the factorials using Sterling's approximation.

$$q_n = \exp\left[-\frac{n(n+1)}{2\omega}\right]. \quad (20)$$

The probability  $p_n$  of obtaining a cycle closure at time  $t = n$  is then

$$p_n = \frac{n}{\omega} q_{n-1} = \frac{n}{\omega} \exp\left[-\frac{n(n+1)}{2\omega}\right]. \quad (21)$$

To obtain  $\mathcal{P}(L)$ , the probability that a given starting point is in the basin of attraction of a cycle of length  $L$ , we note that a closure event at time  $t = n$  yields with equal probability all cycle lengths up to  $n$ . Therefore,

$$\mathcal{P}(L) = \sum_{n=L}^{\infty} \frac{p_n}{n}, \quad (22)$$

which is well approximated by

$$\mathcal{P}(L) \approx \int_{x=L}^{\infty} \frac{1}{\omega} e^{-(x(x+1)/2\omega)} dx \quad (23)$$

$$= e^{1/8\omega} \frac{\pi}{2} \left( \operatorname{Erf} \left( \frac{1+2L}{2\sqrt{2\omega}} \right) \right). \quad (24)$$

Note that the probability distribution of cycle lengths is asymptotically Gaussian (for large lengths), and that the length of a typical cycle is of order  $\sqrt{\omega}$  [5,8]. Derrida [20] has pointed out that the random hopping assumption (or annealed approximation) is exact for the dissipative Kauffman net with  $K = N$ . When  $K < N$ , the random hopping assumption is no longer exact. However, the  $K = N$  results agree well with the simulational data for large but finite  $K$ .

### 3.2.2. Reversible case

As we shall see, the behavior of the reversible model in certain parameter regimes is also well described by a model in which the time development can be considered to be random until a closure event occurs. However, the analysis of  $K = N$  limit is more subtle for the reversible model than for the dissipative case.

#### 3.2.2.1. Wrong calculation: leave out special points.

To illustrate some of the complications that arise when we consider the reversible model, we first present a naive (and wrong) adaptation to the reversible system of the argument in Section 3.2.1. Note that in the reversible models, the state at time  $t$ ,  $\Sigma_t$ , depends on the

spin configurations, or substates, at *two* times,  $\Sigma_{t-1}$  and  $\Sigma_t$ . We once again consider a sequence of states  $\mathcal{S}_0, \mathcal{S}_1, \mathcal{S}_2, \dots$  and *assume* that the map induces “random hopping” through the state space (each  $\mathcal{S}_j$  chosen with equal probability from all allowed possibilities). If the state  $\mathcal{S}_n$  happens to be the same as  $\mathcal{S}_0$ , then the cycle closes with the cycle length being  $L = n$ . Note that at the  $n$ th step there is only one possible output that will give closure,  $\mathcal{S}_n = \mathcal{S}_0$ ; the  $n - 1$  other values of  $\mathcal{S}_j$ ,  $1 \leq j < n$ , are impossible because each cycle must be traversable both forward and backward. Therefore, if the cycle has not closed in the first  $n - 1$  steps, the total number of allowed possibilities for  $\mathcal{S}_n$  is  $\Omega - n + 1$ , of which only one will give closure. This argument yields an estimate for  $\rho_n$ , the probability of closure at the  $n$ th step, given that the orbit has not closed previously:

$$\rho_n = \frac{1}{\Omega - n + 1}. \quad (25)$$

Therefore, this estimate implies that  $p_l$ , the probability that the orbit closes at the  $l$ th step, should be

$$p_l = \rho_l \prod_{k=1}^{l-1} (1 - \rho_k) \quad (26)$$

$$= \frac{l}{\Omega} \quad (27)$$

in the limit of large  $\Omega$ .

These results have been obtained by D’Souza and Margolus [15,24] for a somewhat different class of reversible models. However, for our model, Eq. (27) is wrong. Looking back at Fig. 1, one sees that for  $K = N = 10$ , the average cycle length is of order  $\omega = 2^N \approx 10^3$ . However, Eq. (27) implies an average cycle length of order  $\Omega = 2^{2N} \approx 10^6$ .

**3.2.2.2. A more accurate calculation.** The problem with Eq. (27) is that we have ignored the role of the special points. A sequence of substates of the form

$$\Sigma_{t_1}, \Sigma_{t_1+1}, \dots, \Sigma_{t_1+j}, \Sigma^*, \Sigma^*$$

is reflected at the twin point and *must* continue  $\Sigma_{t_1+j}, \dots, \Sigma_{t_1+1}, \Sigma_{t_1}$ . Similarly, a sequence of substates of the form

$$\Sigma_{t_1}, \Sigma_{t_1+1}, \dots, \Sigma_{t_1+j}, \Sigma^*, \Sigma_{t_1+j+2}, \Sigma^*$$

is reflected at the sandwich point. After the first special point has been hit, the orbit retraces and then continues until a second special point is reached. Once the second special point is reached, say at time  $t = t^*$ , the orbit is reflected again, and closure in less than  $t^*$  additional steps is guaranteed. Since twin points are hit with probability  $1/\omega$  and sandwiches with probability  $m/\omega$  at each time step, this mechanism yields orbit lengths of order  $\omega$  rather than the  $O(\Omega)$  result of Eq. (27).

In the dissipative case discussed above, when  $K = N$ , the calculation of cycle lengths is exact. We have not been able to do that well in the reversible case. However, we present here a simple approximation for the distribution of cycle lengths that is rather accurate when  $\omega$  is large and  $l$  is less than or of the same order as  $\omega$ .

We begin by specifying a realization of the network. Given this realization, we consider a sequence of substates

$$G_l = \Sigma_0, \Sigma_1, \Sigma_2, \dots, \Sigma_l, \Sigma_{l+1} \quad (28)$$

produced by the map. We define a *regular sequence* to be one which has neither closed nor reached a special point. A regular sequence can be used to construct a part of either a regular or a special cycle. We define the sequence (28) to be a sequence of length  $l$ . Given a regular sequence  $G_l$ , we may produce a  $G_{l+1}$  by evolving  $G_l$  for another step. We define the probability  $q(l)$  as the fraction of the realizations in which  $G_{l+1}$  is also a regular sequence and the probability  $\rho(l)$  as the fraction in which it is not.

We take  $G_l$  as a regular sequence and now imagine calculating the next substate  $\Sigma_{l+2}$ . As an approximation, assume that *all*  $\Sigma_{l+2}$  appear with equal probability,  $1/\omega$ . The probability that  $\Sigma_{l+2} = \Sigma_{l+1}$  (i.e.,  $\Sigma_{l+1}$  is a twin point) is  $1/\omega$ , and the probability that  $\Sigma_{l+2} = \Sigma_l$  (i.e.,  $\Sigma_{l+1}$  is a sandwich point) is  $m/\omega$ . There is also a chance  $1/\omega$  that  $\Sigma_{l+2} = \Sigma_0$ . In this last case, the orbit will close with no special points if, in addition,  $\Sigma_{l+3} = \Sigma_1$ . Thus, this estimate yields a probability of closure without special points that is of order  $1/\Omega$ , as in our naive estimate above.

Therefore,  $\rho(l)$ , the probability of a closure event at step  $l$ , given that the sequence has not closed previ-

ously, is the sum of two terms: the probability for closure to a regular sequence  $\rho^R \approx 1/\Omega$ , and the probability of getting a special point  $\rho^S \approx (m+1)/\omega$ , so that

$$\rho(l) = \rho^R(l) + \rho^S(l) \approx \frac{m+1}{\omega}. \quad (29)$$

In addition to ignoring the possibility that  $\Sigma_{l+2}$  has already appeared in the sequence, we have ignored terms of relative order  $1/\omega$ . This is quite reasonable for large  $N$ .

Now we can derive expressions for the number of cycles of different types. There are  $\Omega$  different starting configurations for sequences. We require that the first substate  $\Sigma_0$  not be a sandwich substate and that the second substate  $\Sigma_1$  not be equal to  $\Sigma_0$ . Therefore, the fraction of sequences of the form  $\Sigma_0, \Sigma_1$  (e.g.,  $l = 0$ ) that are regular is  $(1 - 1/\omega)(1 - m/\omega) \sim (1 - (m+1)/\omega)$ . Each iteration reduces the fraction of sequences that are regular by a factor of  $1 - \rho$ , until after  $l$  steps we find that the number of regular sequences,  $N_{RS}(l)$ , is (where again we disregard terms of relative order  $l/\omega$  and smaller)

$$N_{RS}(l) = \Omega \left(1 - \frac{m+1}{\omega}\right) (1 - \rho)^l \approx \Omega e^{-(m+1)l/\omega}. \quad (30)$$

Since the probability of closure to a regular cycle is  $1/\Omega$ , the probability that a randomly chosen point in the phase space is part of a regular cycle that closes in  $l$  steps,  $P_R(l)$ , is  $P_R(l) = N_{RS}(l)/\Omega$ . Because each cycle of length  $l$  is found by starting at any of  $l$  points on the cycle, the average number of regular cycles which close after  $l$  steps is

$$N_R(l) = \frac{N_{RS}(l)}{\Omega l} \approx l^{-1} e^{-(m+1)l/\omega}. \quad (31)$$

A very small proportion of the points in the state space are, in fact, parts of regular cycles. The number which take part in regular cycles of all lengths,  $M_R$ , is

$$M_R = \sum_{j=0}^{\infty} j N_R(j) \approx \frac{\omega}{m+1}. \quad (32)$$

This number is indeed much smaller than the state space volume  $\Omega$ .

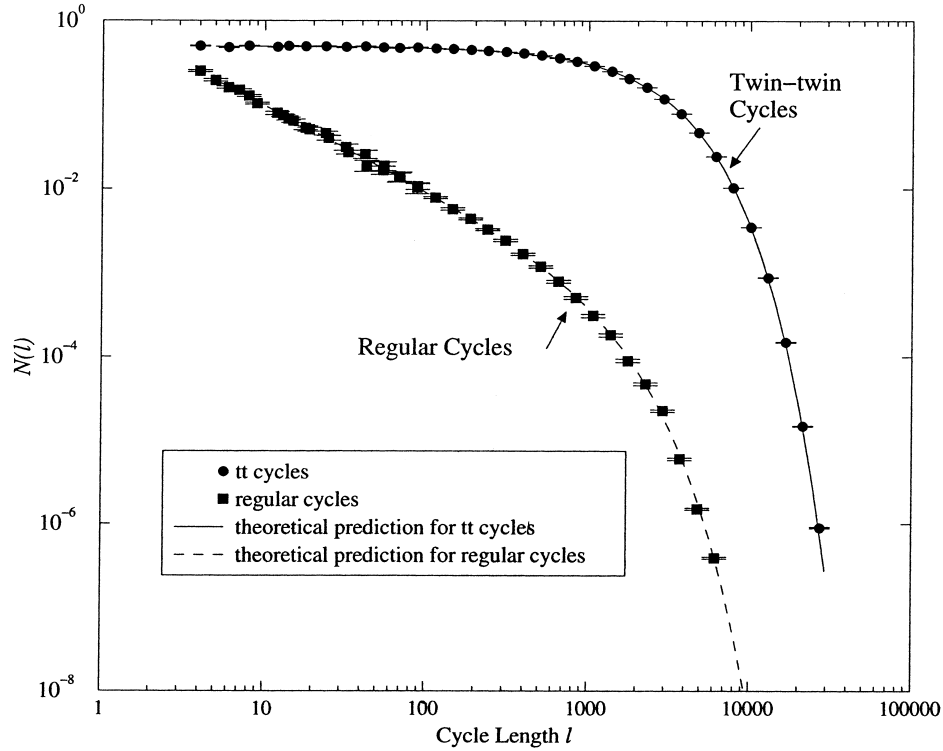


Fig. 2.  $N(l)$  as a function of  $l$ , where  $N(l)$  is the number of cycles of length  $l$ , averaged over realizations. The curves are the results of the random hopping approximation (Eqs. (31), (33a)–(33c)) and the points are simulation data. Simulation results are plotted after being averaged over 10,000 realizations with  $K = N = 10$  and  $m = 0$ .

We now turn our attention to the special cycles, which dominate the state space in this high  $K$  limit. All of them can be found by starting at a special point and iterating until a second special point is reached after  $l$  steps. Then the orbit reverses itself and closes after an additional  $l$  steps. There are three kinds of special cycles, twin–twin, sandwich–sandwich, and twin–sandwich. There are  $\omega m$  different ways to choose the initial point if it is a sandwich point and  $\omega$  ways to choose it if it is a twin point, so the number of twin–twin cycles and sandwich–sandwich cycles of length  $l$  are:

$$N_{\text{tt}}(l) = \frac{1}{2} e^{-(m+1)l/2\omega}, \quad (33a)$$

$$N_{\text{ss}}(l) \approx \frac{1}{2} m^2 e^{-(m+1)l/2\omega}. \quad (33b)$$

The factors of two arise in Eqs. (33a)–(33c) because each cycle of these types is found twice by this method.

Similarly, the number of odd (sandwich–twin) special cycles is

$$N_{\text{st}}(l) \approx m e^{-(m+1)l/2\omega}. \quad (33c)$$

Note that this estimate for the distribution of special cycle lengths depends exponentially on  $l$ , in contrast to the Gaussian dependence for the dissipative model.

To check these conclusions, we plot in Fig. 2,  $N(l)$ , the number of cycles of length  $l$  as a function of  $l$  averaged over realizations. The realizations used all had  $m = 0$ . The theoretical estimates (Eqs. (31), (33a)–(33c)) agree very well with the numerical results. The agreement between the random hopping approximation and the simulation results is equally good for other  $m$ .

**3.2.2.3. Average over  $m$ .** Our results of Eqs. (31), (33a)–(33c) depend upon the number of sandwich

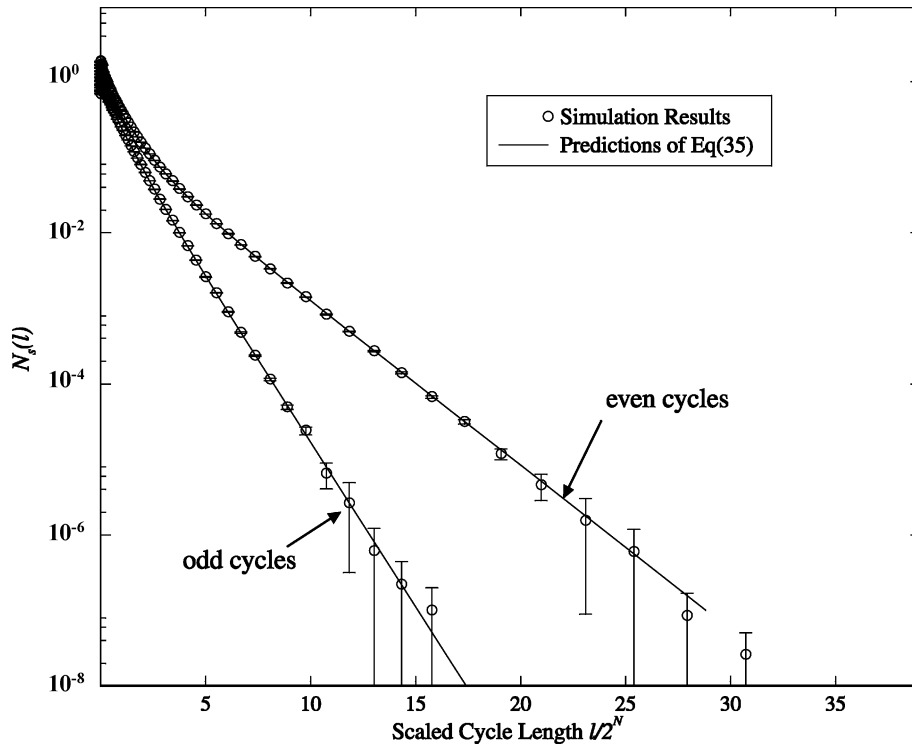


Fig. 3. The average number of special cycles of length  $l$ ,  $N_S(l)$ , plotted against scaled cycle length  $l/2^N$ . The result is averaged over 10,000 randomly selected realizations for  $K = N = 10$  and hence is an average over  $m$ . For each realization, all special cycles were enumerated. The symbols are the results of the simulations. The theoretical results for  $N_S(l)$  obtained from Eqs. (35a)–(35d) are included as solid lines.

special points,  $m$ . In this section, we shall denote averages over  $m$  by  $\langle \cdot \rangle$ . In Appendix A, we show that for  $K = N$ , the probability distribution for  $m$  is a Poisson distribution

$$\rho(m) = \frac{e^{-\lambda} \lambda^m}{m!} \quad \text{with } \lambda = 1. \quad (34)$$

Averaging Eq. (31) using the weight defined in Eq. (34) gives that the realization average of the number of regular cycles of length  $l$ ,  $\langle N_R(l) \rangle$ , is

$$\langle N_R(l) \rangle = l^{-1} \exp \left[ (e^{-l/\omega} - 1) - \frac{l}{\omega} \right]. \quad (35a)$$

Similarly, for the various kinds of special cycles,

$$\langle N_{tt}(l) \rangle = \frac{1}{2} \exp \left[ (e^{-l/2\omega} - 1) - \frac{l}{2\omega} \right], \quad (35b)$$

$$\langle N_{ts}(l) \rangle = \exp \left[ (e^{-l/2\omega} - 1) - \frac{l}{\omega} \right], \quad (35c)$$

$$\langle N_{ss}(l) \rangle = \frac{e^{-l/2\omega} + 1}{2} \exp \left[ (e^{-l/2\omega} - 1) - \frac{l}{\omega} \right]. \quad (35d)$$

To test Eqs. (35a)–(35d) against simulations, in Fig. 3, we plot  $N_S(l)$ , the number of special cycles averaged over realizations, against  $l$ . As discussed in Section 2.2, special cycles formed by two twin points or two sandwich points have an even length, while the ones with one twin point and one sandwich point have an odd length. Therefore,  $N_S(l) = \langle N_{ss}(l) \rangle + \langle N_{tt}(l) \rangle$  if  $l$  is even and  $N_S(l) = \langle N_{ts}(l) \rangle$  if  $l$  is odd. We find that  $N_S(l)$  oscillates because of this difference between even cycle lengths and odd cycle lengths, leading to a two-branch structure in  $N_S(l)$ . This structure was indeed observed in our simulations.

The random hopping analysis of the  $K = N$  situation gives a Hamming distance behavior which is exactly the same in the dissipative [5] and reversible systems. In both cases, the systems start from a pair of configurations which differ in the value of one spin at time  $t$ . By the next time step, the configuration will be random, so that half the spins will be “wrong”. Thus,

the Hamming distance immediately comes to the value  $\frac{1}{2}N$ , and stays there.

#### 4. Intermediate $K$

Section 3 outlines both qualitative and quantitative pictures of the limiting cases  $K = 0$  and  $N$ . In this

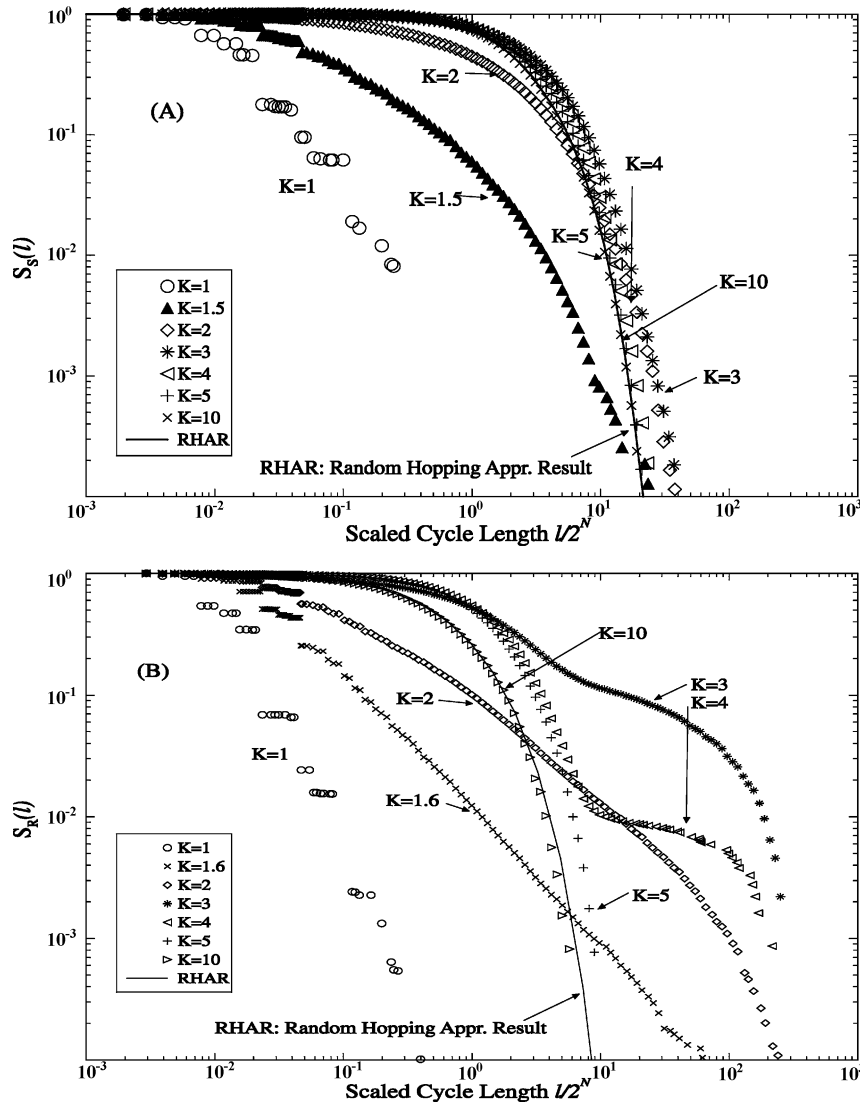


Fig. 4. The plot of survival functions of scaled cycle length  $\hat{l} = l/2^N$  for both special and regular cycles for various  $K$  values and  $N = 10$ : (A) shows the survival function for special cycles,  $S_S(l)$ , and (B) shows the survival function for regular cycles,  $S_R(l)$ . The functions were averaged over 25,600 realizations for each  $K$  value. The survival functions converge to the random hopping case for larger  $K$  values. However, a qualitative theory is still needed to predict the function forms for small  $K$ .

section, we will discuss the system's behavior for intermediate  $K$  values. As  $K$  is increased, there is an evolution from dynamically independent clumps of spins to a situation in which there is random hopping over the whole state space.

Fig. 4 shows numerical results of  $S_S(l)$  and  $S_R(l)$ , the survival functions for special cycles and regular cycles separately for various intermediate  $K$  values. Recall that a survival function of cycle length  $l$  is defined to be the probability of observing cycles with length greater than  $l$  (see Eq. (5)). Non-integer values of  $K$  are produced by mixtures of spins with the neighboring integer  $K$ -values. The survival functions for special cycles,  $S_S(l)$ , as shown in Fig. 4(A), shows no surprising structure. As  $K$  decreases from 2, the observed cycle lengths get shorter and shorter. For  $K \geq 3$ , the survival probabilities approach in a uniform manner the result of Eqs. (35a)–(35d). The reg-

ular cycles are different. For  $K > 5$ , we see a uniform approach to the  $K = N$  result. At  $K = 1.6$ , there seems to be a power law behavior with  $S_R(l) \sim l^{-1}$ . Then for larger values of  $K$ ,  $S_R(l)$  seems to decrease faster than the power law. Finally,  $K = 3$  and 4 show a remarkable bump at large values of  $l/2^N$ , indicating that there is a new process going on at large  $l$ .

The difference between Fig. 4(A) and (B) implies that the relative importance of the two pieces of cycle-closing mechanism depends strongly on  $K$ . Moreover, the relative numbers of regular and special cycles are also strongly  $K$ -dependent. This point is illustrated in Fig. 5, which shows the ratio of the number of regular cycles to that of special cycles as a function of  $K$ . For small  $K$ , several subsets of the spins may become uncoupled, and most cycles are regular cycles. Conversely, special cycles are more likely for large  $K$ .

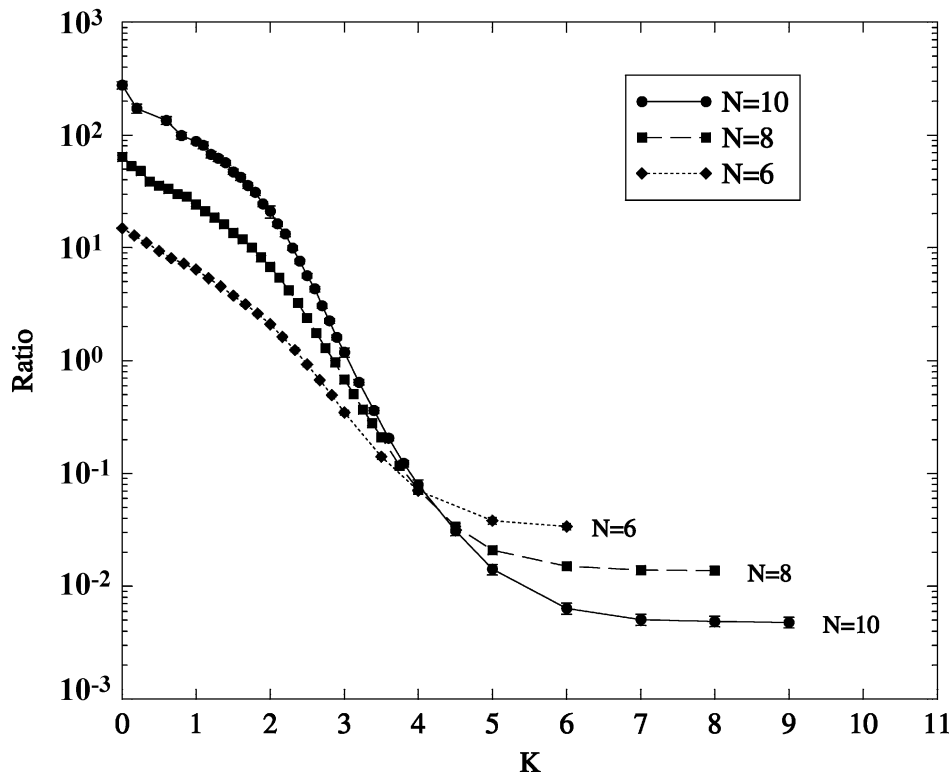


Fig. 5. The ratio of the number of regular cycles to the number of special cycles for  $N = 6, 8$ , and 10. Both the numerator and denominator are averaged over 25,600 realizations. At small  $K$ , there are many more regular cycles than special cycles; at large  $K$ , most of the cycles are special.

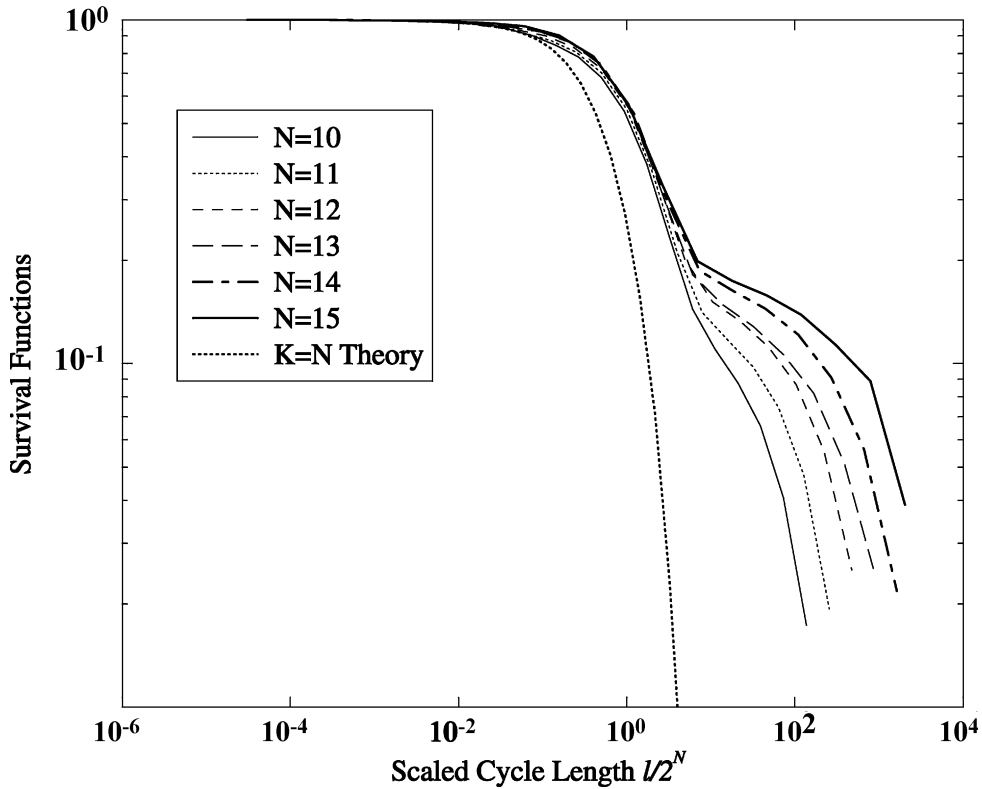


Fig. 6. Plot of  $S_R(l)$  against  $\hat{l} \equiv l/2^N$  for  $K = 3$  and various  $N$ . The drop of  $S_R(l)$  corresponding to the relatively short cycles scale as  $2^N$ , which supports the argument that they are due to special points.

#### 4.1. Anomalously long regular cycles for intermediate $K$ values

Notice the bump in Fig. 4(B) for  $K = 3$  and 4 in the region  $1 \ll \hat{l} \ll \omega$ . This bump arises from a group of regular cycles which are anomalously long. More careful study shows that in fact regular cycles split into two groups, which scale differently. To demonstrate this effect, we plot in Fig. 6 the survival functions  $S_R(l)$  for  $K = 3$  and for a range of  $N$  values against the cycle length  $l$  normalized by  $2^N$ . Manifestly, the distribution of short cycles scales with  $\omega = 2^N$ . This scaling can be explained in the following way. There are  $(m+1)2^N$  special points in the state space of the system, as discussed in Section 2.3. To obtain a regular cycle, the system must not hit any of the special points. The probability of hitting a special point  $\sim (\frac{1}{2})^N$ , so the lengths of the regular cycles scale as  $2^N$ . For

a more explicit and quantitative reasoning, we may appeal to the regular cycle result based on the random hopping assumption described by Eqs. (35a)–(35d), which provides a reasonably accurate approximation of the system when the system is sufficiently well connected. Note that in Eqs. (35a)–(35d), the regular cycle distribution clearly scales as  $2^N$ .

While we have presented an intuitive explanation for the scaling of the relatively short regular cycles, one may still wonder why there is a population of anomalously long cycles and why it appears and disappears as  $K$  increases. To attack these issues, a number of realizations which produce extra long cycles were studied and similarities among them were observed. In general, a realization and the initial configuration have to satisfy the following two conditions to be able to generate an anomalously long cycle: The realization should not have any sandwich points, thereby an-

nulling the mechanism to close a cycle using them, and the functions assigned to the spins together with the choice of initial configurations should prevent a system from hitting a twin point. For small  $K$  values, one can easily find realizations without any sandwich points. For instance, if any spin is assigned the function that is “ $-1$ ” for all inputs, then the realization has no sandwich points. In fact, in Appendix A, we prove that almost all realizations have no sandwich points for finite  $K$  and large enough  $N$  ( $\gg 2^{2^K}$ ).

The twin points in the cycle could be avoided in many ways. For example, when a function assigned to a spin equals to the constant  $+1$ , if this spin starts from  $\sigma_0 = +1$  and  $\sigma_1 = -1$ , it will follow the progression of  $+1, -1, +1, -1, \dots$ , and the system never hits a twin point since  $\sigma_t \neq \sigma_{t+1}$  always holds. Since there is a probability  $(\frac{1}{2})^{2^K}$  that any given spin is assigned the function “ $+1$ ”, and a probability  $\frac{1}{2}$  that this spin starts with  $\sigma_0 = -\sigma_1$ , the probability  $p_2$  that at least

one spin is in the “ $+ - + -$ ” progression is

$$p_2 = 1 - \left(1 - \left(\frac{1}{2}\right) \left(\frac{1}{2^{2^K}}\right)\right)^N \approx 1 - \exp\left(-\frac{N}{2^{(2^K-1)}}\right) \quad (2^{2^K} \gg 1). \quad (36)$$

Thus, when  $N \gg 2^{2^K}$ , almost all starting configurations and realizations will not hit a twin point.

Another way to avoid twin points consists of two spins that are assigned identical inputs and functions. In this case, it is possible to choose an initial configuration for these two spins, which will stop the system from forming a twin point. For instance, a system in which spin 1 and spin 2 are assigned identical input spins and functions starting from  $\sigma_{t=0}^1 = \sigma_{t=1}^1 = 1$  and  $\sigma_{t=0}^2 = -1, \sigma_{t=1}^2 = 1$  can never hit a twin point. It is also easy to prescribe certain simple progressions for a few spins and stop the system from hitting a

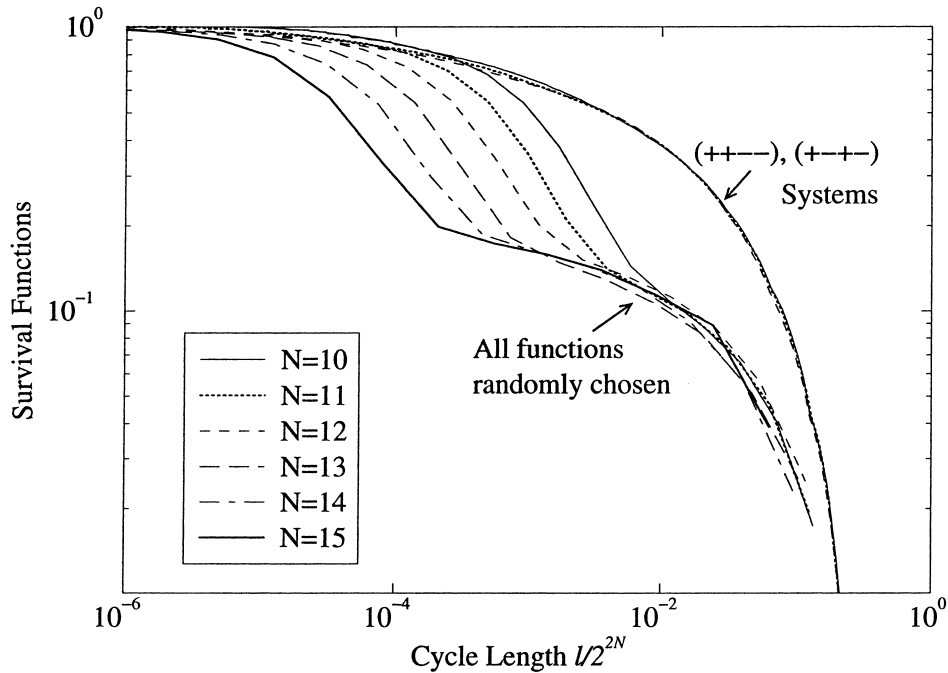


Fig. 7. Survival functions of regular cycle lengths in systems with all functions chosen at random as well as systems with one spin assigned the function  $-1$  and a second spin assigned the function  $+1$  and initial condition  $(+1, -1)$ , plotted against  $l/2^{2N}$  for various  $N$  and for  $K = 3$ . As expected, the lengths of anomalously long cycles in the systems with randomly functions, as well as all the cycles in the  $(+, +, -, -), (+, -, +, -)$  systems, scale approximately as  $2^{2N}$ .

twin point. For example, two spins both with period 3 evolving following the pattern,

$$\sigma_0 : + + - + + - + + - \dots ,$$

$$\sigma_1 : - + + - + + - + + \dots$$

can prevent the system from forming a special cycle.

The mechanisms preventing the system from hitting a twin point always appear to be related to some small piece of the system that evolves independently from other parts of the system. The couplings are such that this piece is not affected by anything outside itself (though in general it can and does affect the rest of the system). We call a piece like this a local structure. Local structures are to be discussed in detail in the next paper in this series. Note that local structures are very unlikely for sufficiently large  $K$  values, where the spins of the system are quite correlated, unless  $N$  is enormous. When  $K$  is small, local structures occur

much more frequently. When many a local structures are present, almost all the realizations and initial configurations have no special points. Thus, the presence of local structures leads to very long regular cycles. Since for a given  $N$ , the local structures become less probable as  $K$  increases, it is natural to find the number of regular cycles decreases as  $K$  increases.

Section 3.2.2 presents a naive theory of hopping in state space that ignores the role of the special points and predicts that the distribution of orbit lengths in a system of  $N$  spins should scale as  $2^{2N}$ . This naive theory fails qualitatively when  $N = K$  because the special points induce orbit closure in order  $2^N$  steps. However, if local structures prevent the system from ever reaching a special point, then the mechanism for closing the orbits in order  $2^N$  steps does not operate and it is plausible that the typical orbit lengths will be much longer than  $2^N$ . We test this idea by calculating orbit lengths in systems

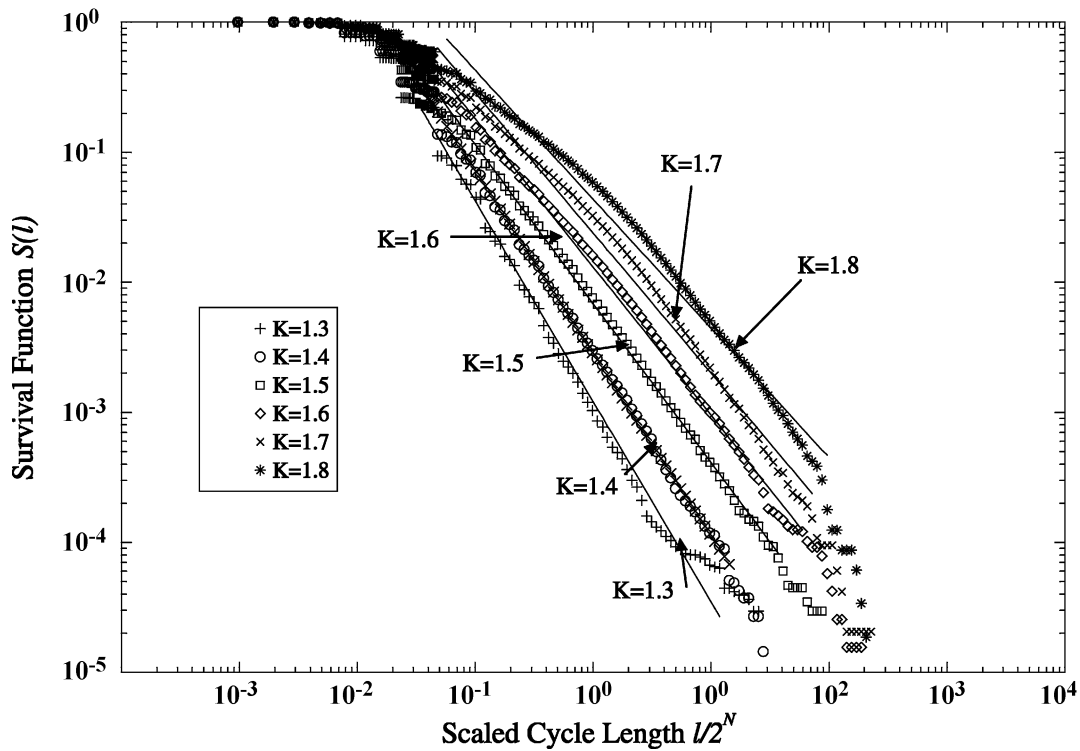


Fig. 8. Survival functions of regular cycle lengths plotted against  $l/2^N$  for various  $K$  values and for  $N = 10$ . The solid lines are the power law fits for the survival functions. By inspection, one can see for  $K \in [1.4, 1.7]$  the survival functions follow power law fairly well for three decades.

with one spin assigned the function  $-1$  (so it follows the sequence  $(+1, +1, -1, -1, +1, +1, \dots)$ ) and a second individual spin assigned the function  $+1$  and the initial condition  $(+1, -1)$  (so its evolution is  $(+1, -1, +1, -1, \dots)$ ). Such  $(+, +, -, -)$ ,  $(+, -, +, -)$  systems can never reach a special point. As Fig. 7 demonstrates, in these systems orbit lengths grow with  $N$  much faster than  $2^N$ ; the numerical results are consistent with  $2^{2N}$  scaling.

We believe that the orbit lengths in systems with  $N \gg 2^{2^k}$  and randomly chosen functions cannot grow faster than  $2^{2N(1-\epsilon(K))}$ , where  $\epsilon(K)$  is of order  $2^{-2^k}$ . This is because of order  $N2^{-2^k}$  spins have input functions  $1$  or  $-1$  and hence cycle with periods  $1, 2$ , and  $4$ . More generally, we expect interesting crossover phenomena to occur when  $K$  is both large and of the order of  $\log_2(\log_2 N)$ . Even for  $K = 3$ , simulating systems with large enough  $N$  to permit numerical exploration of these effects is computationally prohibitive.

#### 4.2. Average cycle length versus $N$ for different values of $K$

When  $K$  is large, the random hopping approximation works well and the cycle length distribution scales as  $\omega = 2^N$ . Fig. 4 demonstrates that the distribution of cycle lengths does not change dramatically while  $K$  decreases until  $K$  is quite small. Therefore, it is reasonable to expect the average cycle length to increase exponentially with  $N$  when  $K$  is large. On the other hand, when  $K = 0$ , the average cycle length is bounded above by  $4$ . For  $K = 1$ , our simulations and analytic arguments indicate that it scales as  $\log N$ ; the results will be presented in the companion publication. For values of  $K$  in the range  $[1.4, 1.7]$ , the survival functions  $S(l)$  decay roughly as a power law over three decades in cycle length  $l$ , as shown in Fig. 8. This result is consistent with the presence of a phase transition. The companion paper on the behavior of the Hamming distance presents more compelling evidence for a phase transition at  $K \approx 1.6$ .

## 5. Summary

This paper addresses the dynamics of a Boolean network model of  $N$  elements with  $K$  inputs with

time-reversible dynamics. We present the general setup of the model and introduce the concept of special points and the distinction between special cycles and regular cycles. The relation between special points and the properties of the cycles is demonstrated. We show that the numbers of special points and special cycles for each realization are proportional to  $\omega \equiv 2^N$ , where  $N$  is the number of variables in the system.

We determine the probability distribution of cycle lengths as well as the survival functions. In the limiting case  $K = 0$ , the cycle length is bounded above by  $4$  and the probability that a cycle length is  $4$  approaches  $1$  as  $N$  increases. For  $K = N$ , within a random hopping approximation, we calculate the survival functions for regular cycles and for special cycles, which agree with simulational data extremely well.

Finally, we present the simulational results for survival functions for intermediate  $K$  values. A population of anomalously long regular cycles scaling as  $2^{2N}$  is found for small  $K$  values and explained based on the notions of special points and local structures. The correlation between typical cycle length and the  $K$  values of the networks is studied, and we find that the typical cycle length increases logarithmically with  $N$  when  $K < 1.4$ , exponentially when  $K > 1.7$ , and following a power law when  $K$  falls in between; these results are compatible with the presence of a phase transition for  $K$  somewhere in the range of  $[1.4, 1.7]$ .

## Acknowledgements

SNC and LPK gratefully acknowledge financial support from the MRSEC program of the National Science Foundation under Award Number DMR9808595.

## Appendix A. Some statistical properties of sandwich points

The text discusses twin and sandwich symmetry points which induce closure of orbits in the reversible Kauffman model. Each type arises when the substate  $\Sigma_t$  is such that each of the functions of these inputs takes on a target value. For a twin point,  $\sigma_{t+1}^j = \sigma_t^j$ , so the target function is different at every time step. For a

sandwich point, for all  $t$  the target function is  $F^i = 1$  for every  $i$ .

To calculate orbit lengths, we need to compute the probability that a symmetry point of either type occurs at each time  $t$ . For a given realization of couplings, the number of substates for which the functions take on a particular value can vary. Because the target value for the twin point is different for different substates, whereas the target values for the sandwich points are the same at all times, the statistics of the two types of symmetry points are different.

The process we consider is one in which couplings and an initial condition are chosen, and then the system evolves in time. We assume that this time evolution yields a random sampling of all possible spin configurations or substates. At each time  $t$ , we examine whether a symmetry point of either type has been reached. Let  $m$  be the number of substates for which  $F^j = 1$  for all  $j$  (the criterion for a sandwich point), and  $m_t$  be the number of spin configurations for which each function takes on the target value for a twin point at time  $t$ . At a time  $t$ , the probability of being at a twin point is  $m_t/\omega$ , whereas the probability of being at a sandwich point is  $m/\omega$ . On average, it takes many trials before a special point is reached; the probability of having observed a twin point after  $T$  trials  $\approx \sum_{t=1}^T m_t/\omega \approx \langle m \rangle T/\omega = T/\omega$ , where  $\langle \rangle$  is the average over realizations, whereas the probability of having observed a sandwich symmetry point is  $mT/\omega$ .

We wish to calculate the probability that a randomly chosen realization has a given value of  $m$ . Now each output takes on a given value with probability  $\frac{1}{2}$ , so on average the probability that  $N$  outputs all have given target values is  $(\frac{1}{2})^N$ , implying that the realization average  $\langle m \rangle = 2^{-N}$ . However, if one of the functions happens to be  $F^i = -1$ , then clearly there are no sandwich points. We wish to find  $P_K(m)$ , the fraction of all possible realizations of the couplings for a given  $K$  that yield each value of  $m$ .

First we consider  $K = N$ . This case is particularly relevant because when  $K$  is large, essentially all the orbits close because of the symmetry points. Here, the functions can be viewed as mapping a given input substate into a randomly chosen output substate. Since there are  $\omega = 2^N$  possible output substates, of which

one is the target, each input configuration has a probability  $1/\omega$  of having its output be the target.  $P_{K=N}(0)$ , the probability that no input configurations has as its output the target configuration, is  $(1 - 2^{-N})^{2^N}$ , which, as  $N \rightarrow \infty$ , approaches  $1/e$ . The probability that exactly one of the  $2^N$  different inputs yields the target output is  $(2^N)(2^{-N})(1 - 2^{-N})^{2^N - 1} \rightarrow 1/e$ . Similarly,  $P_{K=N}(m)$ , the probability that exactly  $m$  of the  $2^N$  different inputs yields the target output is

$$P_{K=N}(m) = \frac{(2^N)!}{m!(2^N - m)!} (2^{-N})^m (1 - 2^{-N})^{2^N - m} \\ \rightarrow \frac{1}{m! e} \quad (N \rightarrow \infty, m \ll 2^N). \quad (\text{A.1})$$

Thus,  $P_{K=N}(m)$  is a Poisson distribution. Since  $P_{K=N}(m)$  falls off quickly as  $m$  gets large, clearly it is consistent to assume that  $m \ll 2^N$ .

However, when  $K$  is finite and  $N$  is large enough, we expect the behavior of  $P_K(m)$  to differ qualitatively from the  $K = N$  result. We expect that almost all configurations will have  $m = 0$  for any finite  $K$  as  $N \rightarrow \infty$ . We have argued before that if in a realization a spin is assigned a function that equals to constant  $-1$ , the realization has no sandwich point. Also, if two spins are assigned functions  $F^1$  and  $F^2$  such that

$$F^1 + F^2 = 0$$

for all inputs, there can be no sandwich point for the realization. There are many other possible mechanisms that lead to  $m = 0$ . Clearly, the probability that a realization has at least one spin function of  $-1$  bounds below the probability that it has no sandwich point. Among  $2^{2^K}$  possible functions that can be assigned to one spin, one is  $-1$  for all inputs. Assuming that all functions are equally likely to be picked and that the function choices for different spins are independent, the probability that no spin is assigned the constant function  $-1$  is

$$\left(1 - \frac{1}{2^{2^K}}\right)^N \approx \exp\left(-\frac{N}{2^{2^K}}\right) \quad (N \gg 2^{2^K}).$$

Thus,  $P_K(m = 0)$  is bounded by the probability that the realization has at least one function that is  $-1$ , or  $P_K(m = 0) \geq (1 - \exp(-N/2^{2^K}))$ . This result implies that whenever  $K$  is finite, in a large enough

system sandwich points cause orbit closure only in a vanishingly small fraction of realizations. However, when  $K$  is not small, realizations with sandwich points are rare only when  $N$  is enormous (when  $N \gg 2^{2^K}$ ).

## Appendix B. Relation between special points and cycles

Here, we prove the results used in Section 2 that (1) each special cycle contains exactly two special points, (2) cycles with two special points of the same kind have even cycle lengths, and (3) cycles with different kinds of special points have odd lengths.

To prove that each special cycle contains two and only two special points, we first consider a cycle of even length  $2n$ ,

$$\Sigma_0, \Sigma_1, \dots, \Sigma_{2n-1}.$$

Suppose there is a twin point in the cycle. By relabeling the cycle, we can get

$$\Sigma_{n-1} = \Sigma_n$$

by definition. Now  $\Sigma_{n-1-t} = \Sigma_{n+t}$  since the cycle is time reversible, so that  $\Sigma_0 = \Sigma_{2n-1}$  when we take  $t = n - 1$ . Thus, we find another twin point in this even-length cycle. If there is a sandwich point at  $n$ , then

$$\Sigma_{n-1} = \Sigma_{n+1},$$

and  $\Sigma_{n-1-t} = \Sigma_{n+1+t}$ , thus

$$\Sigma_1 = \Sigma_{2n-1}.$$

Here, we find another sandwich point at 0. Similarly, when the cycle is odd, we will find a twin point in the presence of a sandwich point, and vice versa.

By now, we have proven that if there is a special point in the cycle, then there has to be another. The statement that the cycle length being odd or even depends on whether the special points are of the same kind, is also clear from the above argument.

To finish the proof, we need to demonstrate that no orbit can contain more than two special points. Assume that an orbit of length  $L$  with more than two

special points exists. Choose the origin of time so that  $\Sigma_{L-j} = \Sigma_j$  (one does this by placing a sandwich substate at  $t = 0$  or placing twin substates at  $t = 1$  and  $t = L$ ), and let  $P$  be the smallest value for which  $\Sigma_{P-n} = \Sigma_{P+n}$  for all  $n$ ;<sup>4</sup> by assumption,  $P < \frac{1}{2}L$ . Then, we must have simultaneously  $\Sigma_{L-j} = \Sigma_j$  and  $\Sigma_{P-n} = \Sigma_{P+n}$ . Letting  $j = P - n$  yields  $\Sigma_{L-P+n} = \Sigma_{P-n} = \Sigma_{P+n}$ . Letting  $q = P + n$ , we obtain  $\Sigma_{L-2P+q} = \Sigma_q$ . Thus, the orbit period is  $L - 2P$ , which is strictly less than  $L$ , so we have a contradiction.

We can also show that these two special points must be different from one another. Suppose not. Consider an orbit of length  $L$ , and choose the origin of time so that  $\mathcal{S}_0$  and  $\mathcal{S}_P$  are the same special point, with, by assumption,  $P < L - 1$ . Applying the map yields  $\mathcal{S}_j = \mathcal{S}_{(P+j)}$  for any  $j$ , so the orbit repeats after  $P$  steps. But this contradicts the assumption that  $L$  is strictly greater than  $P$ .

## References

- [1] J.H. Kaufman, D. Brodbeck, O.M. Melroy, Critical biodiversity, *Conserv. Biol.* 12 (3) (1998) 521–532.
- [2] B. Derrida, Dynamics of automata, spin glasses and neural networks, Notes for School at Nota, Sicily, 1987.
- [3] S. Kauffman, *At Home in the Universe: The Search for Laws of Self-organization and Complexity*, Oxford University Press, Oxford, 1995.
- [4] S. Kauffman, Emergent properties in random complex automata, *Physica D* 10 (1–2) (1984) 145–156.
- [5] S. Kauffman, *The Origins of Order: Self-organization and Selection in Evolution*, Oxford University Press, Oxford, 1993.
- [6] H. Flyvbjerg, N.J. Kjær, Exact solution of Kauffman's model with connectivity one, *J. Phys. A* 21 (7) (1988) 1695–1718.
- [7] U. Bastolla, G. Parisi, Closing probabilities in the Kauffman model: an annealed computation, *Physica D* 98 (1) (1996) 1–25.
- [8] U. Bastolla, G. Parisi, Relevant elements, magnetization and dynamical properties in Kauffman networks: a numerical study, *Physica D* 115 (3–4) (1998) 203–218.
- [9] U. Bastolla, G. Parisi, The modular structure of Kauffman networks, *Physica D* 115 (3–4) (1998) 219–233.
- [10] A. Bhattacharjya, S.D. Liang, Power-law distributions in some random Boolean networks, *Phys. Rev. Lett.* 77 (8) (1996) 1644–1647.

<sup>4</sup> If the special point at  $P$  is a twin point, then  $2P$  is odd, otherwise it is even.

- [11] L. Glass, C. Hill, Ordered and disordered dynamics in random networks, *Europhys. Lett.* 41 (6) (1998) 599–604.
- [12] M. Mezard, G. Parisi, M.A. Virasoro, *Spin Glass Theory and Beyond*, World Scientific, Singapore, 1987.
- [13] B. Derrida, D. Stauffer, Phase-transitions in two-dimensional Kauffman cellular automata, *Europhys. Lett.* 2 (10) (1986) 739–745.
- [14] S.K. Ma, *Modern Theory of Critical Phenomena*, Benjamin, Reading, PA, 1976.
- [15] R.M. D’Souza, Ph.D. Thesis, Massachusetts Institute of Technology, Massachusetts, 1999 (Chapter 8).
- [16] T. Toffoli, N.H. Margolus, Invertible cellular automata: a review, *Physica D* 45 (1990) 229–253.
- [17] G.D. Birkhoff, *Dynamical Systems*, American Mathematical Society, Providence, RI, 1927.
- [18] J.M. Greene, *J. Math. Phys.* 9 (1968) 760.
- [19] S.C. Shenker, L.P. Kadanoff, *J. Stat. Phys.* 27 (1982) 631.
- [20] B. Derrida, H. Flyvbjerg, Multivalley structure in Kauffman model — analogy with spin-glasses, *J. Phys. A* 19 (16) (1986) 1003–1008.
- [21] B. Derrida, Valleys and overlaps in Kauffman’s model, *Phil. Mag.* 56 (6) (1987) 917–923.
- [22] M.D. Stern, Emergence of homeostasis and noise imprinting in an evolution model, *Proc. Natl. Acad. Sci. USA* 96 (19) (1999) 10746–10751.
- [23] B. Luque, R.V. Sole, Phase transitions in random networks: simple analytic determination of critical points, *Phys. Rev. E, Part A* 55 (1) (1997) 257–260.
- [24] R.M. D’Souza, N.H. Margolus, Thermodynamically reversible generalization of diffusion limited aggregation, *Phys. Rev. E* 60 (1) (1999) 264–274.
- [25] J.M. Greene, *J. Math. Phys.* 20 (1979) 1183.